AUTOMATED DETECTION OF PITTED CONES AND IMPACT CRATERS: DEEP-LEARNING APPROACH FOR SEARCHING POTENTIAL HYDROTHERMAL ACTIVITY AND RELATED ORE DEPOSITS ON MARS.

B. Pieterek[1], M. Grochowski[2], J. Ciążela[3], O. Sokolov[2], and M. Józefowicz[4]; [1]Institute of Geology, Adam Mickiewicz University, ul. Bogumiła Krygowskiego 12, 61-680 Poznań, Poland, barpie@amu.edu.pl, [2]Faculty of Physics, Astronomy and Informatics, Nicolaus Copernicus University in Toruń, ul. Grudziądzka 5, 87-100 Toruń, grochu@is.umk.pl, [3]Institute of Geological Sciences, Polish Academy of Science, ul. Podwale 75, 50-449 Wrocław, Poland, j.ciazela@twarda.pan.pl, [4]European Space Foundation, Grodzka 42/1, 31-044 Kraków, Poland, m.jozefowicz@spacefdn.com

Introduction and background information: The growing number of images acquired by the Martian satellites together with Deep Learning algorithms caused development of automated approaches for searching various landforms on Mars. Since 2006, with the start of the *Mars Reconnaissance Orbiter* (MRO) mission, we are constantly receiving high-resolution images of Mars's surface. The MRO Context Camera (CTX) is currently orbiting Mars and acquiring gray-scale images at a resolution of ~5 m/pixel [1]. CTX provides geological context and distinguishes critical future science targets for two other MRO instruments, the High Resolution Imaging Science Experiment (HiRISE) and Compact Reconnaissance Imaging Spectrometer for Mars (CRISM). Above 90,000 CTX images have already covered the entire planet. This high number of images is difficult to process for the small planetary remote sensing community

Therefore, automated detection methods have been rapidly employed, most of all for the identification of impact craters [2,3] and block falls [4]. In Deep Learning, the popularity of Convolutional Neural Networks (CNNs) is still increasing as an alternative to manual mapping and analyzing visual imagery. The major advantage of CNNs compared to other image classification algorithms is their independence from prior knowledge and human intervention in feature extraction as CNNs use automated learning for filter optimization. A comprehensive study of recent CNNs applications and advantages was provided by DeLatte at al. [2]. CNNs have been already successfully used on Mars for the automated detection of geological landforms such as volcanic rootless cones and transverse aeolian ridges by Palafox et al. [5]. They have shown that CNNs have better precision and recall in testing data than traditional classifiers based on Support Vector Machines (SVMs).

In the last decades, the cone-like structures on Mars garnered interest [6,7 and references therein]. In some cases, the origin of these structures is still discussed [8], but two major types include volcanic (e.g., scoria cones, rootless cones, and phreatomagmatic tuff cones) and sedimentary (e.g., mud volcanoes). Although the cones of different origins show various morphological characteristics [6,8,9], after their identification on the surface of Mars, more detailed studies are needed to fully reconstruct their origin (e.g., spectral analysis of CRISM [8,10]). Common involvement of water (groundwater or permafrost) and heat released by volcanic activity (e.g., magma chamber, lava flows) during cone formation may result in the activation of hydrothermal circulation in the vicinity of the cone-like structures [11]. For example, on Mars, the hydrothermal mineralization associated with scoria cones has been already documented by Brož et al. [10] within the Coprates Chasma volcanic field. Whereas the formation of scoria, rootless, or tuff cones is related to the interaction between magma/lava and groundwater, likely resulting in high-temperature fluid circulation, on Earth, the mud volcanism might be also controlled by the heat released from magma intrusion accompanied by low-temperature hydrothermal circulation [12,13]. In addition, some cone-like structures on Mars might be formed by the hydrothermal venting as suggested by Lanz and Saric [14]. The hydrothermal circulation can also be triggered by moderate or large impact events (craters >5–10 km diameter) [15,16].

Therefore, mapping pitted cone fields of various origins and large impact craters is crucial to provide
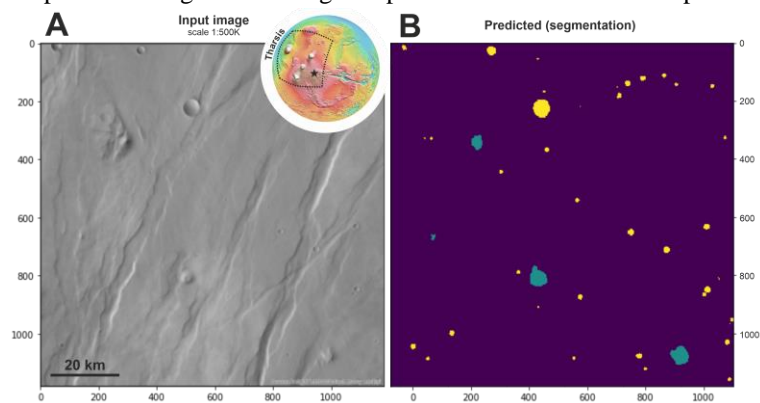

Figure 1: (A) Testing image of an unnamed area located near Noctis Fossae [7]. The marker on the insert shows the location of testing area on the topographic map of Mars. **(B)** The post processing map showing segmentation results with the morphological features classified into classes such as pitted cones (green), impact craters (yellow), and background (violet).

more constraints on hydrothermal and related ore-forming processes on Mars. To reduce the mapping time of these landforms, we have developed an automated algorithm for searching and identifying cone-like structures and impact craters on Mars using Convolutional Neural Networks on the CTX global mosaic of Mars.

Method: We used the preliminary CTX image mosaic (beta01 version) created by the Caltech Bruce Murray Laboratory (available at: http://murray-lab.caltech.edu/CTX/). All images applied for training and evaluation of the code were extracted from the mosaic using ArcMap software on the scale of 1:500,000. To obtain a sufficient number of cone-like structures that can be used for training, we implemented most of the documented Martian volcanic fields of scoria cones such as Ulysses Colles, Hydraotes Colles, Coprates Chasma, and Noctis Fossae [6,7] as well as mud volcanoes of Chryse Planitia [17]. To evaluate the correctness in the identification of cone-like landforms, we tested an unnamed field of pitted cones located to the east of the Noctis Fossae volcanic field. To design our algorithm, we applied four CNN architectures for image segmentation including U-Net [18], fully convolutional network (FCN) [19], pyramid scene parsing network (PSPNet) [20], and SegNet [21]. We compared the segmentation performance of these architectures using several configurations for each of them with various network depths and by applying two types of network backbone, Visual Geometry Group (VGG) and ResNet. These four architectures show near-constant segmentation results with the highest values of validation intersection over union (IOU) parameter for U-Net (0.70) and U-Net with VGG backbone (0.72). The U-Net VGG was used in our final code. To create training data, the original image size (11812x11812 pixels; 1500 dpi) is reduced 10 times and then divided into 480x480 px chunks (25% of the Mars surface overlap for two neighboring pieces). At first, each training image was manually annotated to mark the location of pitted cones, impact craters, and background with three different colors (Fig. 1B) to create a training target for the semantic segmentation task. Due to the limited number of training samples, heavy data augmentation was used to prevent overfitting and increase robustness to noise. During this segmentation, the algorithm identifies the three aforementioned morphological classes. Then the segmented image is filtered to remove artifacts and noise. Finally, the connected component labeling algorithms is performed to extract solid regions and determine their location and size. In addition, at this stage, we have used a filter that removes small objects (<5 pixels in perimeter) from further consideration. After the segmentation and detection process, the code generates a summary table with the location and parameters of the identified objects.

Results and Conclusions: To evaluate our algorithm, we used two testing images on the scale of 1:500,000. Before the segmentation, we did not conduct any manual mapping. The algorithm has detected 8 potential cones and 71 impact craters. In no case, the algorithm has misidentified the cone and impact crater. After the code implementation, we have conducted a detailed manual mapping using the same scale. We have confirmed the cones' origin for all of the mapped structures and identified one additional cone that has not been recognized by the algorithm. Considering impact craters the algorithm did not detect 17 of them, whereas 2 were false detections. Therefore, the success rate for pitted cones and impact craters are ~90% (7/8) and ~80% (71/90), respectively. The designed algorithm efficiently detects most pitted cones and impact craters on the Mars surface. This significantly increases our chances in searching for hydrothermal activity and related ore deposits, which will be crucial in future Mars exploration by humans.

References: [1] Malin, M. C. et al. (2007) *JGR Planets,* 112, 1–25. [2] DeLatte et al. (2019) *IEEE J-STARS,* 12, 2944–2957. [3] Lagain et al. (2021 *Nat. Commun.,* 12, 6352. [4] Fanara et al. (2020) PSS, 180, 104733. [5] Palafox, L. F. et al. (2017) *Comput. Geosci.,* 101, 48–56. [6] Brož, P. et al. (2021) *J. Volcanol. Geotherm. Res.,* 409. [7] Pieterek, B. et al. (2022) *Icarus,* 114851. [8] Dapremont, A. & Wray, J. J. (2021) JGR *Planets,* 126. [9] Farrand, W. H. et al. (2005) *JGR Planets,* 110, 1–14. [10] Brož, P. et al. (2017) *EPLS,* 473, 122–130. [11] West, M. D. & Clarke, J. D. A (2010) *PSS,* 58, 574–582. [12] Malvoisin, B. et al. (2018) *EPLS,* 497, 42–49. [13] Mazzini, A. & Etiope, G (2017) *Earth-Science Rev.* 168, 81–112. [14] Lanz, J. K. & Saric, M. B. (2009) *JGR Planets* 114, 1–13. [15] Schulze-Makuch, D. et al. (2007) *Icarus,* 189, 308–324. [16] Osinski, G. R. et al. (2013) *Icarus* 224, 347–363. [17] Komatsu, G. et al. (2016) *Icarus* 268, 56–75. [18] Ronneberger, O. et al. (2015) *MICCAI.* 9351, 12–20. [19] Long J., at al. (2017) *IEEE TPAMI,* 4, 640–651. [11] Zhao, H. et al. (2017) IEEE CVPR. 2881-2890. [12] Badrinarayanan V. et al. (2017) *IEEE TPAMI,* 39, 12, 2481-2495.